Experimental Investigation Of Heat Transfer In A Rectangular Channel With Perforated Ribs

Mehmet Eren[*,a], Sinan Caliskan[a], Muammer Zırzakıran[b]

[*a]Department of Mechanical Engineering, Hitit University, 19030, Çorum, TURKEY

[b]Vocational College of Erzurum, Atatürk University, ERZURUM
mehmeteren088@gmail.com

Abstract: Ribs are known to enhance the heat transfer between the energy-carrying fluid and the heat transfer surfaces. One effect of surface roughness is to increase momentum transfer and flow resistance. An experimental investigation of forced convection heat transfer in a rectangular channel with perforated ribs is presented. Measurements are carried out for a rectangular channel, rib transverse pitch (S) to transverse rib height (e) ratio of S/e=12.0, and a rib height (e) to channel height (H) ratio of e/H= 0.1. The convective fluid was air, and the Reynolds numbers considered for the channel flow case range from 5375 to 36362. The aim of the work was to study the effect of the thermal performance of the ribbed channel. The heat transfer results were obtained using an infrared thermal imaging technique. The heat transfer results of the perforated ribs are compared with those of a smooth plate. The presence of perforated ribs produces higher heat transfer coefficients than the smooth plate surfaces. Results show a 34.1% increase in heat transfer due to the use of ribs. These perforated ribs show a more significant increase in heat transfer coefficient for channel flows.

Key words: Heat transfer; perforated ribbed channel; thermal imaging technique; Pressure drop

Introduction

Perforated rib arrays inside internal channels are often used in heat exchanger systems to enhance the heat transfer in gas turbine blade cooling channels. A typical application is the internal cooling of gas turbine blade: the ribs break the laminar sublayer and create local wall turbulence due to flow separation and reattachment between the ribs, thus greatly enhancing the cooling effect.

First studies dealt with uniformly heated square or rectangular channels with two opposite rib-roughened walls; continuous, regularly spaced, transverse ribs have been the most common ribbed geometry for years (Han, Glickmann and Rohsenow, 1978 – Han, 1988). The effects of the most important parameters (rib height, rib pitch, channel aspect ratio, hydraulic diameter, and Reynolds number) on heat transfer and pressure drop were investigated. Further studies (Han,Park and Lei, 1985 – Han, Ou, Park and Lei, 1989) showed that the use of parallel angled ribs can have a significant impact on local heat transfer and pressure drop because of the secondary flow induced by the rib angle. To overcome this drawback, modified ribs in the form of "perforated ribs" have been applied instead of solid ones (Liou, Chen, 1998 – Karwa, Maheshwari,Karwa, 2005). Caliskan (Çalışkan, 2013) investigated heat transfer and flow characteristics under impingement of a multiple circular jet array with perforated rib surfaces (PRS) and solid rib surfaces (SRS) with an infrared thermal imaging technique and a Laser-Doppler Anemometry system, respectively.

Perforated ribs have been designed. In order to investigate the convective heat transfer performance of perforated ribs, an experimental set-up was established. The effects of perforated ribs from the channel bottom on the heat transfer and pressure drop characteristics were examined.

Experimental setup

The experimental setup is shown in Fig. 1. The experimental system consisted of a honeycomb, an entrance section, a test section, a centrifugal blower, an infrared thermography system, perforated ribs, and devices for measuring flow velocity, temperature and pressure difference. Air was drawn in by a variable speed fan and passed through the test section of the channel. The channel inner cross section dimensions were 100mm (wide) and 50mm (height). The channel was constructed with 9mm thick plexiglass plates. The dimensions of the heating plate were 100mm (width) and 270mm (length). In the experiments, the heating plate was made of stainless steel foil. It was firmly clamped and stretched between two copper bus bars. The foil was electrically heated by means of a high current DC power supply to provide a constant heat flux surface. The perforated ribs were mounted on the bottom of the channel to enhance the convective heat transfer. The averaged heat transfer coefficient on the plate surface was measured for various rates of airflow through the channel.

Views of perforated ribs are shown in Fig. 2. The perforated ribs were made of high conductivity aluminum material. The perforated ribs were attached to the stainless steel foil plates by a thin layer of super-glue. The thermal contact resistance due to the super-glue introduced a minor conservative preference to the reported results (Rallabandi, Rhee, Gao, Han, 2010). Thermal images were obtained from an IR camera positioned on the bottom of the heater assembly vertical to the z-direction. The air velocity was measured by the Kimo LV107-type anemometer connected to the output of the blower. ALMEMO and a pressure transducer were used to determine the pressure drop between the air inlet and outlet at the test section. The inlet and outlet temperatures of the channel air were measured in different locations of the channel by using a K-type thermocouple. All of these thermocouples were connected to a PC-based data acquisition system. The infrared thermography system, which included a ThermaCAM SC500 camera from FLIR systems and a PC with AGEMA Researcher software, could measure temperatures from -20 ºC to 1200 ºC with an accuracy of ±2%. The infrared camera used an uncooled focal plane array detector with 320x240 pixels, which operated over a wavelength range of 7.5-13 μm . The field of view was 25ºx18.8º/0.4m; the instantaneous field of view was 1.3 m-rad, and the thermal sensitivity was 0.07ºC at 30ºC. The images captured by the infrared camera were displayed and recorded using a computer for further analysis.

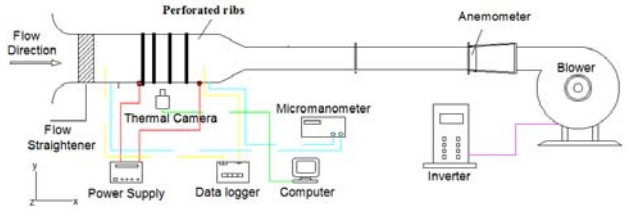

Figure 1: Experimental set-up

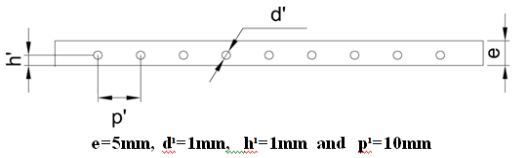

Figure 2: Schematic view of present perforated ribs

The bottom side of the stainless steel foil was covered with a layer of black backing paint. The emissivity of each side of the plate was measured with an AE anemometer and was found to be 0.82 and 0.13 for the painted and unpainted surfaces, respectively.

The local heat transfer coefficient and Nusselt number were defined as:

$$h_x = \frac{q_{conv}}{(T - T_{b,x})} \tag{1}$$

where T and T_{bx} were the local temperature of the heating surface and the bulk fluid, respectively.

$$Nu_x = \frac{h_x D_h}{k} \tag{2}$$

The convective heat flux was evaluated as follows:

$$q_{conv} = \frac{Q_{el} - Q_{loss}}{A} \tag{3}$$

where Q_{el} was the measured input power to the heater. Radiation, free convection from the bottom side, and conduction were considered as heat losses.
The radiation heat flux from both sides of the sheet was given by

$$q_r{}^{front} = \varepsilon_t \sigma\left(T^4 - T_b^4 \right) \tag{4}$$

$$q_r{}^{back} = \varepsilon_b \sigma\left(T^4 - T_\infty^4 \right) \tag{5}$$

where ε_t and ε_b are the emissivities of the unpainted and painted surfaces, respectively. σ is the Stefan-Boltzmann constant.

The free convection heat flux from the bottom side of the sheet was calculated using

$$q_f = h_f \left(T - T_\infty \right) \tag{6}$$

where the free convection coefficient h_f was defined as 1.1 W/m^{2}K, for an air velocity of 0.1 m/s (Janssen, Warmoeskerken, 1991)
The conduction was given by:

$$q_C = k\frac{\Delta T}{t} \tag{7}$$

where k was the thermal conductivity of the sheet, ΔT was the temperature difference across the sheet, and t was the thickness of the sheet. As a result of the thinness of the sheet, the lateral conduction was negligible as reported by Lytle and Webb (Lytle, Webb, 1994). The sum of Q_{loss} was typically in the range of 7.3 to 10.4% of Q_{el} at the highest Reynolds number.

The averaged Nusselt number Nu_{avg} was calculated by integrating the local Nusselt number over the heating surface, i.e.,

$$Nu_{avg} = \frac{1}{L}\int Nu(x)\partial x \tag{8}$$

The Reynolds number based on the channel hydraulic diameter was given by

$$\mathrm{Re} = \frac{\rho u D_h}{\mu} \tag{9}$$

where D_h=2WH/(W+H) was the channel hydraulic diameter.

Friction factor, f, can be written as

$$f = \frac{\Delta P}{\left(\frac{L}{D_h}\right)\rho U^2/2} \tag{10}$$

where Δp was pressure drop across the length of the channel, L.

The experimental uncertainties had been determined by a standard error analysis. Both the inlet and outlet temperatures of the air were measured by using calibrated K-type thermocouples with an accuracy of 0.3 °C. The inlet velocities at the centers were measured by an anemometer with an uncertainty of 0.03 m/s. The uncertainty in the experimental data was determined according to the procedure proposed by Kline and McClintock (Kline, McClintock, 1953). In our experiment, the fluid properties were assumed constant. The uncertainty in the calculation of the Nusselt number and Reynolds number was found to be less than 6.2% and 5.8%, respectively. The uncertainty in the friction factor f was estimated to be 4.2% at the highest Reynolds number and 6.7% at the lowest Reynolds numbers. The maximum uncertainty of the infrared thermography measurements was less than $\pm 1.5\%$.

Results and Discussion

The experimental data for the heat transfer and friction factor in a rectangular duct with perforated ribs was examined under a turbulent flow regime. The present experimental results in a smooth wall channel were first validated in terms of the Nusselt number and the friction factor. The Nusselt number and the friction factor obtained from the present smooth channel were, respectively, compared with the correlations of Dittus-Boelter and Blasius found in the open literature (Incropera, 1996) for turbulent flow in ducts.

Correlation of Dittus-Boelter,

$$Nu = 0.023\,\mathrm{Re}^{0.8}\,\mathrm{Pr}^{0.4} \quad \text{for heating} \tag{11}$$

Correlation of Blasius,

$$f = 0.316\,\mathrm{Re}^{-0.25} \quad \text{for } 3000 \le \mathrm{Re} \le 20{,}000 \tag{12}$$

Fig. 3 and 4 shows, respectively, a comparison of the Nusselt number and the friction factor obtained from the present work with those from correlations of Eqs. (11) and (12). In the figures, the present results reasonably agree well within the ±11.8% deviation for both the friction factor and Nusselt number correlations.

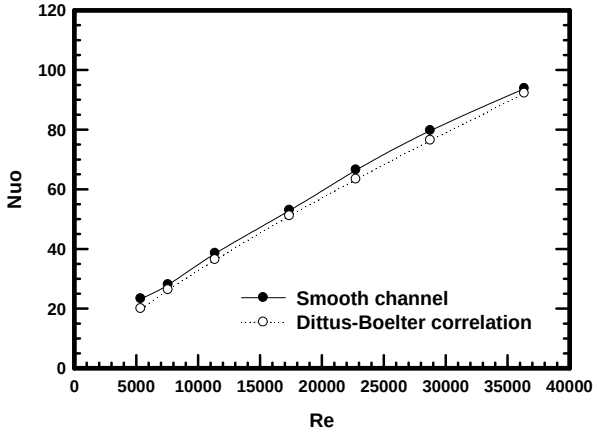

Figure 3: Verification of Nusselt number for smooth channel

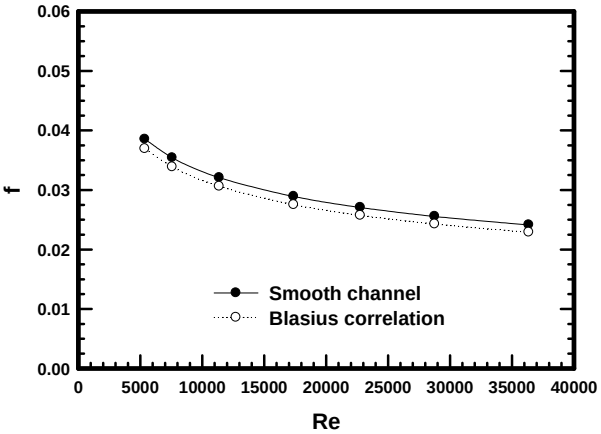

Figure 4: Verification of friction factor for smooth channel

Effects of perforated ribs

The present experimental results on heat transfer characteristics, in a channel equipped with perforated ribs are presented in the form of Nusselt number. The Nusselt numbers obtained under turbulent flow conditions for perforated ribs with different Reynolds number are presented in Fig. 5. As shown in Fig. 5, the use of perforated ribs lead to considerable heat transfer enhancements in a similar trend in comparison with the smooth channel and the Nusselt number values, increase with the rise of the Reynolds number. The maximum difference of the averaged Nusselt number the between smooth and perforated rib is found to occur at Re=36362 with a value equal to 34.1%.

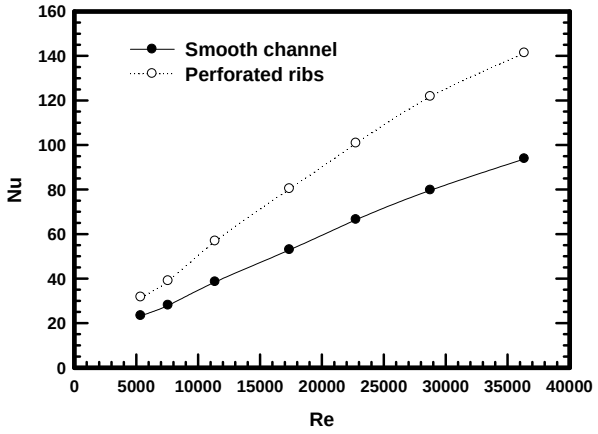

Figure 5: Variation of avareged Nusselt number with Reynolds number

Fig. 6a, b and c present the temperature contours for the perforated ribs in both the streamwise and the spanwise directions for the different Reynold number. As shown in Fig. 6a, b and c, the temperature is decreases with increasing of the Reynolds number. The wall temperatures for the perforated rib surface were lower than the smooth surface, which disrupted the boundary layer more, resulting in a better heat transfer.

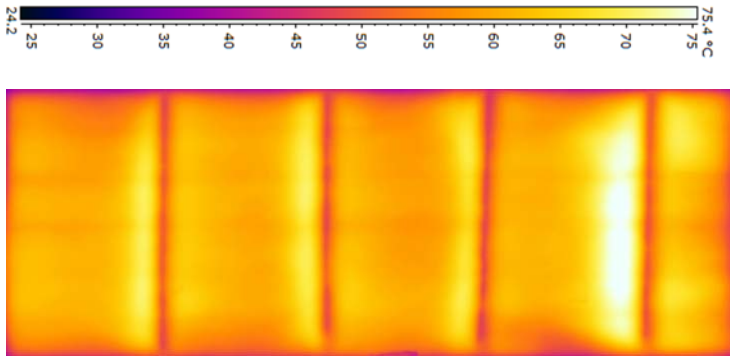

(a) Re=5375

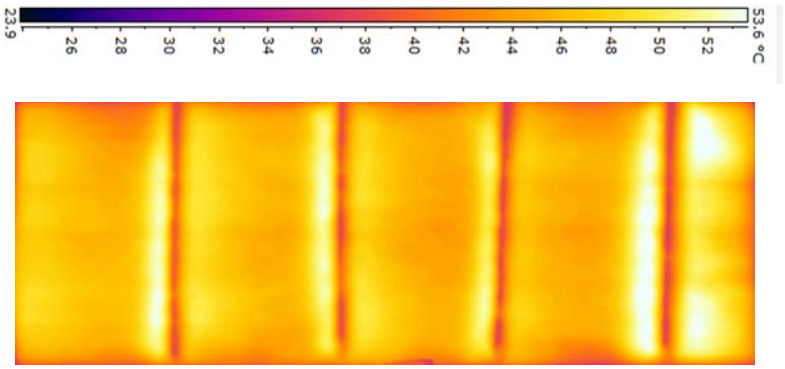

(b) Re=17390

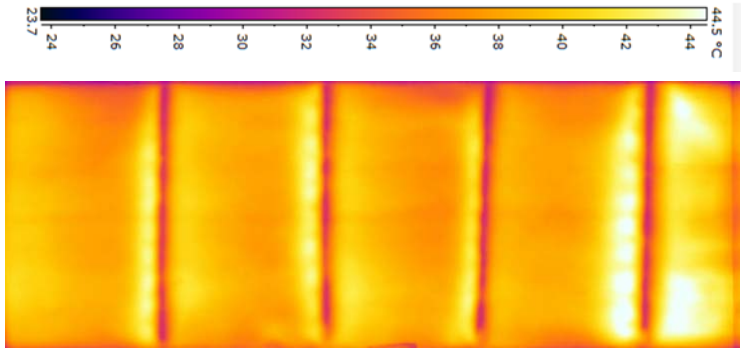

(c) Re=36362

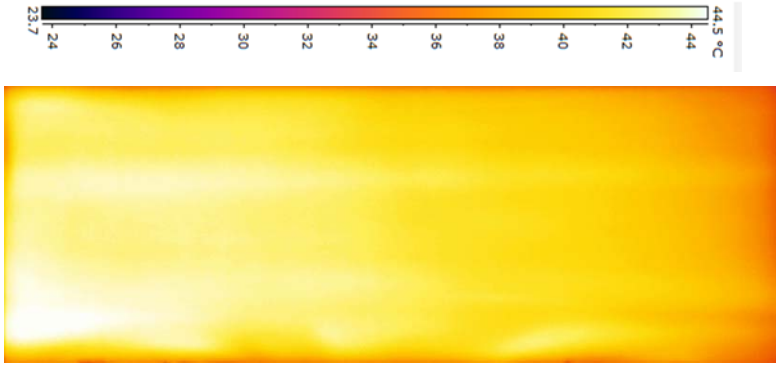

(d) Re=36362

Figure 6: Temperature contours in the x-y plane for the perforated ribs and smooth surface **(a)** Re=5375-perforated ribs, **(b**) Re=17390-perforated ribs **(c)** Re=36362-perforated ribs and **(d)** Re=36362 smooth surface.

Variations of the ratio friction factor, f, versus the Reynolds number for the perforated ribs are shown in Fig. 7. The friction factor found from using the perforated ribs was observed to be higher than that from the smooth duct. This can be attributed to flow blockage and the act caused by the reverse flow due to the presence of the perforated ribs.

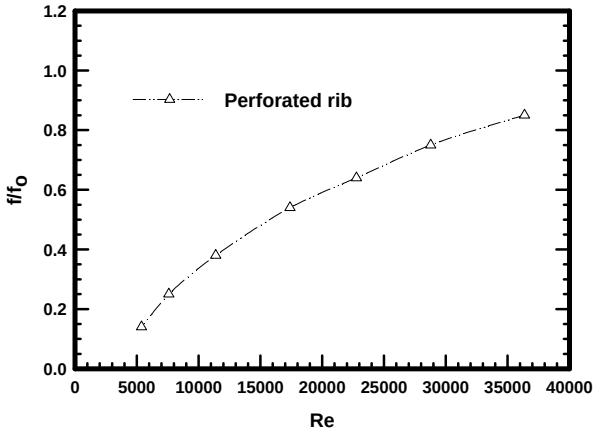

Figure 7: Friction factor ratio with Reynolds number

Conclusions

An experimental investigation in a rectangular duct with perforated ribs under uniform heat flux conditions has been performed.

The following conclusions have been drawn:

- Perforated ribs had significantly enhanced the heat transfer rate, in comparison to a smooth duct. The averaged heat transferred from surfaces with perforated ribs was higher than that of the smooth surface. The disturbance in the boundary layer was formed due to holes, which created higher turbulence due to the separated and reattached flows.
- The present results reasonably agree well within the ±12% deviation for both the friction factor and Nusselt number correlations.
- The maximum difference of the averaged Nusselt number the between smooth and perforated rib is found to occur at Re=36362 with a value equal to 34.1%.

Acknowledgements

The present work is financially supported by the Hitit University (Grant No.MUH01.13.010).

Nomenclature

A	convection heat transfer area of channel (m^2)
D_h	hydraulic diameter (m)
f	friction factor (-)
H	channel height (m)
h	averaged heat transfer coefficient (W/m^2 K)
k	thermal conductivity of air (W/m K)
Nu	Nusselt number (-)
Nu_{avg}	averaged Nusselt number (-)
ΔP	pressure drop (Pa)
Pr	Prandtl number (-)
Re	Reynolds number (-)
Q	heat transfer (W)
T	temperature (K)
U	mean velocity (m/s)

Greek symbols

ρ	density of the fluid (kg/m^3)
ν	kinematic viscosity (m^2/s)

References

Buchlin, J.M. (2002). Convective heat transfer in a channel with perforated ribs, *International Journal Thermal Science 41* (pp.332–340).

Çalışkan, S. (2013). Flow and heat transfer characteristics of transverse perforated ribs under impingement jets, *International Journal of Heat and Mass Transfer 66* (pp.244-260).

Han, J.C., Glickmann, L.R. and Rohsenow, W.M. (1978). An Investigation of Heat Transfer and Friction for Rib-Roughened Surfaces, *Int.J. Heat Mass Transfer*, vol.21, (pp.1143-1156).

Han, J.C. (1983). Enhanced Heat Transfer in a Flat Rectangular Duct With Streamwise-Periodic Disturbances at One Principal Wall, *ASME Journal of Heat Transfer*, vol.105, (pp.851-861).

Han, J.C. (1984). Heat Transfer and Friction in Channels With Two Opposite Rib-Roughened Walls, *ASME Journal of Heat Transfer*, vol.106, (pp.774-781).

Han, J.C., Park, J.S. and Lei, C.K. (1985). Heat Transfer Enhancement in Channels With Turbulence Promoters, *ASME Journal of Eng. for Gas Turbines and Power*, vol.107, (pp.628-635).

Han, J.C. (1988). Heat Transfer and Friction Characteristics in Rectangular Channels With Rib Turbulators, *ASME Journal of Heat Transfer*, vol.110, (pp.321-328).

Han, J.C. and Park, J.S. (1988). Developing Heat Transfer in Rectangular Channels With Rib Turbulators, *Int.J. Heat Mass Transfer*, vol.31, (pp.183-195).

Han, J.C., Ou, S., Park, J.S. and Lei, C.K. (1989). Augmented Heat Transfer in Rectangular Channels of Narrow Aspect Ratios With Rib Turbulators, *Int.J. Heat Mass Transfer*, vol.32, (pp.1619-1630).

Hwang, J.J.,Lia, T.Y., Liou, T.M. (1998). Effect of fence thickness on pressure drop and heat transfer in a perforated-fenced channel, *International Journal of Heat and Mass Transfer 41* (pp.811–816).

Incropera, F., Dewitt, P.D. (1996). *Introduction to Heat Transfer, 3rd edition*, NY: John Wiley &Sons Inc

Janssen, L.P.B.M., Warmoeskerken, M.M.C.G. (1991).*Transport Phenomena-Data Companion*. DUM, Delft, 2

Karwa, R., Maheshwari, B.K., Karwa, N. (2005). Experimental study of heat transfer enhancement in an asymmetrically heated rectangular duct with perforated baffles, *International Communications in Heat and Mass Transfer 32* (pp.275–284).

Kline, S.J., McClintock, F.A. (1953). Describing uncertainties in single-sample experiments, *Mechanical Engineering 73* (pp.3-8).

Liou, T.M., Chen, S.H. (1998). Turbulent heat and fluid flow in a passage disturbed by detached perforated ribs of different heights, *International Journal of Heat and Mass Transfer 41* (pp.1795–1806).

Lytle, D., Webb, B.W. (1994). Air Jet Impingement Heat Transfer at Low Nozzle Plate Spacings, *Int. J. Heat Mass Transfer 37* (pp.1687-1697).

Rallabandi, A.P., Rhee, D.H., Gao, Z., Han, J.C. (2010). Heat transfer enhancement in rectangular channels with axial ribs or porous foam under through flow and impinging jet conditions, *International Journal of Heat and Mass Transfer 53* (pp.4663-4671).

Sara, O.N., Pekdemir, T., Yapici, S., Yilmaz, M. (2001). Heat-transfer enhancement in a channel flow with perforated rectangular blocks, *International Journal Heat and Fluid Flow 22* (pp.509–518).

Sparrow, E.M. and Tao, W.Q. (1983). Enhanced Heat Transfer in a Flat Rectangular Duct With Streamwise-Periodic Disturbances at One Principal Wall, *ASME Journal of Heat Transfer*, vol.105, (pp.851-861).